Dhaka Univ. J. Sci. 59(1): 125-130, 2011 (January)

Dynamics of Three Dimensional Lorenz Equations

Md. Shahidul Islam and Mir Shariful Islam
Department of Mathematics, Dhaka University, Dhaka, Dhaka - 1000, Bangladesh
E-mail: mshahidul11@yahoo.com

Received on 15. 04. 2010. Accepted for Publication on 01. 08. 2010

Abstract

In this paper, we investigate the Lorenz attractor and its dynamical behavior. We discussed the strange attractor, as its chaotic behavior. These behaviors are analyzed in analytically, numerically and graphically. The results are compared with behavior for a couple of other strange attractors. Mathematica are used to solve the model and sketch the graphical solution of chaotic and non-chaotic behavior.

I. Introduction

The Lorenz equations are a set of three ordinary differential equations modeling convection rolls in the atmosphere that appear as warm air rises into cooler layers of air at higher altitude. This set of equations was originally proposed by Edward Lorenz in 1963. Lorenz[1], a meteorologist as well as a Mathematician, derived by introducing a truncation to the Navier-Stokes equation[2] effectively reducing it to a set of three ordinary differential equations in 3-dimensional space. The non-linear equations are

$$\frac{dX}{dt} = \sigma Y - \sigma X$$
$$\frac{dY}{dt} = rX - XZ - Y$$
$$\frac{dZ}{dt} = XY - bZ$$

where $X(t)$ is the rate of convective overturning, $Y(t)$ is the horizontal temperature variation, and $Z(t)$ is the vertical temperature variation. The parameter r is proportional to the Rayleigh number, b is dependent on the geometry of the cell and the parameter σ is proportional to the Prandtl number, which is the ratio of the fluid viscosity to the thermal conductivity for a given fluid. The properties of the system, which is originally used to model fluid circulation in atmosphere, is the subject of dynamical systems and chaos theory.

The equations are derived as a simplification of Saltzman's (1962) non-periodic model for convection. For the Earth's atmosphere, typical values for parameters are σ=10, r = 28 and b = 8/3, and the initial point is (10, 0, 10). If this system is perturbed slightly, the general form will remain. Like the weather, this system is highly sensitive to its initial conditions. This characteristic is also sometimes used in turbulence. A small difference in initial conditions would yield a small difference in results, except near unstable equilibrium.

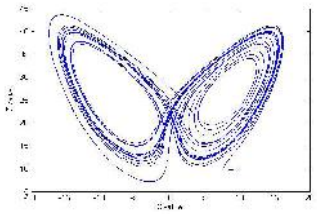

Fig. 1. A numerical solution of the Lorenz equations projected onto the X-Z plane showing non-periodic behavior

Two trajectories begin with very close initial conditions, in particular, $X_1 = X_2 = 10$, $Y_1 = Y_2 = 0$, $Z_1 = 10$, $Z_2 = 10.000000001$. For the first 25 time units, the two trajectories seem identical. However, beyond 30 time units, they seem completely unrelated to each other.

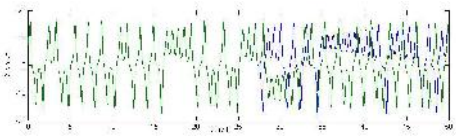

Fig. 2. Two numerical solutions of the Lorenz equations showing sensitivity to initial conditions

Due to the non-linearity of the equations, an exact form of the solution can't be calculated. The Runge-Kutta method is one of the most well known numerical methods for the differential equations of order four and five. The numerical methods, such as Euler's and Runge-Kutta methods are calculated approximation to the system of solution through iteration[3]. We show that the modified fifth order Runge-Kutta method are able to solve the Lorenz model and compare the solution between methods on chaotic and non-chaotic model.

II. Runge-Kutta Method

The modified fifth-order Runge-Kutta HaM-RK5[5] methods[4] were done by substituting the arithmetic mean in the stages. The formula is presented as:

$$y_{n+1} = y_n + h(b_1k_1 + b_2k_2 + b_3k_3 + b_4k_4 + b_5k_5)$$

where

$$k_1 = f(x_n, y_n)$$
$$k_2 = f(x_n + ha_2, y_n + ha_2k_1)$$
$$k_3 = f(x_n + ha_3, y_n + ha_3\frac{k_1 + k_2}{2})$$
$$k_4 = f(x_n + ha_4, y_n + ha_4\frac{k_1 + k_2 + k_3}{2})$$
$$k_5 = f(x_n + ha_5, y_n + ha_5\frac{k_1 + k_2 + k_3 + k_4}{2})$$

b_1, b_2, b_3, b_4 and b_5 are the weight chosen so that the parameter a_1, a_2, a_3, a_4 and a_5 can be determined and $\frac{1}{n}\sum_{i=1}^{n} k_i$ is defined as the arithmetic mean. For simplicity of the algebra, we consider f as a function of y, without loss

of generality. This will reduce the Taylor series expansions of k_i, $i = 1,2,3,4,5$ to the following:

$$k_1 = f,$$

$$k_2 = f + fha_2 f_y + \frac{1}{2} f^2 h^2 a_2^2 f_{yy},$$

$$k_3 = f + \frac{1}{2} ha_3 f_y (2f + fha_2 f_y + \frac{1}{2} f^2 h^2 a_2^2 f_{yy}) + \frac{1}{8} h^2 a_3^2 f_{yy} (2f + fha_2 f_y + \frac{1}{2} f^2 h^2 a_2^2 f_{yy})^2,$$

$$k_4 = f + \frac{1}{3} ha_4 f_y (3f + fha_2 f_y + \frac{1}{2} f^2 h^2 a_2^2 f_{yy}) + \frac{1}{2} ha_3 f_y (2f + fha_2 f_y + \frac{1}{2} f^2 h^2 a_2^2 f_{yy}) + \frac{1}{8} h^2 a_3^2 f_{yy} (2f + fha_2 f_y + \frac{1}{2} f^2 h^2 a_2^2 f_{yy})^2 + ...$$

$$k_5 = f + \frac{1}{4} ha_5 f_y (4f + fha_2 f_y + \frac{1}{2} f^2 h^2 a_2^2 f_{yy}) + \frac{1}{2} ha_3 f_y (2f + fha_2 f_y + \frac{1}{2} f^2 h^2 a_2^2 f_{yy}) + \frac{1}{8} h^2 a_3^2 f_{yy} (2f + fha_2 f_y + \frac{1}{2} f^2 h^2 a_2^2 f_{yy})^2 + \frac{1}{3} ha_4 f_y (3f + fha_2 f_y + \frac{1}{2} f^2 h^2 a_2^2 f_{yy}) + \frac{1}{2} ha_3 f_y (2f + fha_2 f_y + \frac{1}{2} f^2 h^2 a_2^2 f_{yy}) + \frac{1}{8} h^2 a_3^2 f_{yy} (2f + fha_2 f_y + \frac{1}{2} f^2 h^2 a_2^2 f_{yy})^2 + \frac{1}{18} h^2 a_3^2 f_{yy} (3f + fha_2 f_y + \frac{1}{2} f^2 h^2 a_2^2 f_{yy}) + \frac{1}{2} ha_3 f_y (2f + fha_2 f_y + \frac{1}{2} f^2 h^2 a_2^2 f_{yy}).$$

Taylor series expansion of y_{n+1} can be written as

$$y_{n+1} = y_n + hf + \frac{1}{2} h^2 ff_y + \frac{1}{6} h^3 (ff_y^2 + f^2 f_{yy}) + \frac{1}{24} h^4 (f^3 f_{yyy} + ff_y^3 + 4f^2 f_y f_{yy}) + ...$$

comparing the coefficients of the terms up to h^5, some equations which are used to determine the parameters $b_1, b_2, b_3, b_4, b_5, a_2, a_3, a_4, a_5$ are obtained and solved using Mathematica 5.2 software. It can be represented by

$$y_{n+1} = y_n + h(b_1 k_1 + b_2 k_2 + b_3 k_3 + b_4 k_4 + b_5 k_5)$$

where

$$k_1 = f(x_n, y_n)$$

$$k_2 = f(x_n + ha_2, y_n + ha_2 k_1)$$

$$k_3 = f(x_n + ha_3, y_n + ha_3 \frac{k_1 + k_2}{2})$$

$$k_4 = f(x_n + ha_4, y_n + ha_4 \frac{k_1 + k_2 + k_3}{2})$$

$$k_5 = f(x_n + ha_5, y_n + ha_5 \frac{k_1 + k_2 + k_3 + k_4}{2}).$$

We attained two sets of solution:

RK5[1]: $a_4 = 0.1$ and $a_5 = 0.1$,

$b_1 = -3.7783286500685627, b_2 = -0.18312885616492072,$

$b_3 = 0.04837565197099888, b_4 = -17.700904612988186,$

$b_5 = 22.61398646725067, a_2 = 0.6826487126671337$

and $a_3 = 2.7638749083367884$.

The second set is,

RK5[2]: $a_4 = 0.5$ and $a_5 = 0.5$,

$b_1 = 0.17604368301238185, b_2 = 0.1535302041097001,$

$b_3 = -0.3333576978522315, b_4 = 1.1214760294680406,$

$b_5 = -0.11769221873789096, a_2 = -0.9869797512962593$

and $a_3 = -0.4488850808987729$.

Table. 1. *x*-direction differences among all methods for *r* = 23.5

t	*x*		
	RK5[1]$_{0.01}$-RK5[1]$_{0.001}$	RK5[2]$_{0.01}$-RK5[2]$_{0.001}$	HaM-RK5[5]$_{0.01}$-HaM-RK5[5]$_{0.001}$
0	0.00E+00	0.00E+00	0.00E+00
0.1	5.66E-02	1.92E-01	1.15E+00
0.2	2.21E-02	7.95E-02	2.16E+00
0.3	5.04E-03	1.24E-02	2.96E+00
0.4	7.38E-03	2.03E-02	3.69E+00
0.5	6.77E-02	2.33E-03	4.92E+00
0.6	1.25E-02	4.39E-02	5.96E+00
0.7	1.12E-02	3.44E-02	3.89E+00
0.8	1.95E02	7.00E-02	3.13E+00
0.9	2.86E-02	9.68E02	6.97E+00
1	1.70E-02	5.48E-02	2.40E+00

III. Results and Discussions

To solve the Lorenz system where σ and *b* are set to be 10 and 8/3 respectively which the initial conditions is given by *x*(0) = -15.8, *y*(0) = - 7.48 and *z*(0) = 35.64. The fifth-order methods were examined in time range [0, 1] with two time steps Δt = 0.01 and Δt = 0.001.

For *r* = 23.5, we determine the accuracy of RK5[1], RK5[2] and HaM-RK5[5] with time steps Δt = 0.01 and Δt = 0.001. The results are presented in Tables 1-3 and the corresponding graph in Figs. 1-3.

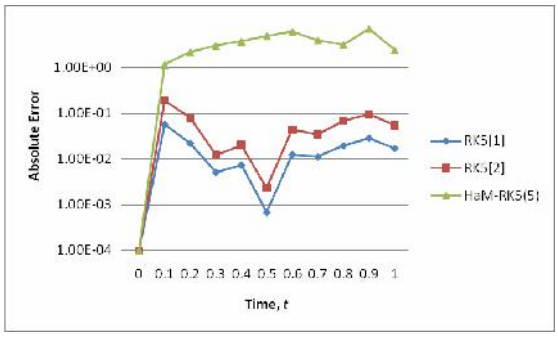

Fig. 1. Absolute error of all methods for x

Table. 2. y-direction differences among all methods for $r = 23.5$

t	y		
	$RK5[1]_{0.01}$-$RK5[1]_{0.001}$	$RK5[2]_{0.01}$-$RK5[2]_{0.001}$	HaM-$RK5[5]_{0.01}$-HaM-$RK5[5]_{0.001}$
0	0.00E+00	0.00E+00	0.00E+00
0.1	4.51E-02	1.52E-01	4.83E+00
0.2	1.62E-02	5.35E-02	3.66E+00
0.3	1.02E-02	3.14E-02	3.49E+00
0.4	2.44E-03	3.69E-03	4.67E+00
0.5	8.88E-03	3.41E-02	6.37E+00
0.6	2.01E-02	6.64E-02	6.28E+00
0.7	1.06E-02	4.31E-02	6.63E-01
0.8	4.04E-02	1.38E-01	1.06E+01
0.9	2.14E-02	6.83E-02	5.85E+00
1	3.91E-02	8.39E-03	2.97E+00

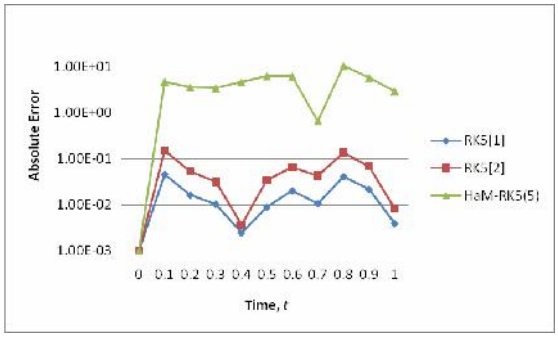

Fig. 2. Absolute error of all methods for y

Table. 3. z-direction differences among all methods for $r = 23.5$

t	z		
	$RK5[1]_{0.01}$-$RK5[1]_{0.001}$	$RK5[2]_{0.01}$-$RK5[2]_{0.001}$	HaM-$RK5[5]_{0.01}$-HaM-$RK5[5]_{0.001}$
0	0.00E+00	0.00E+00	0.00E+00
0.1	5.79E-02	2.05E-01	1.78E-01
0.2	3.23E-02	1.15E-01	1.40E+00
0.3	2.15E-02	7.52E-02	1.55E-01
0.4	2.21E-02	7.30E-02	1.74E+00
0.5	1.87E-02	5.63E-02	4.98E+00
0.6	6.77E-03	3.18E-02	1.05E+01
0.7	3.79E-02	1.28E-01	1.46E+01
0.8	1.78E-03	1.83E-03	5.93E+00
0.9	3.35E-02	1.18E-01	8.29E+00
1	4.11E-02	1.40E-01	8.66E+00

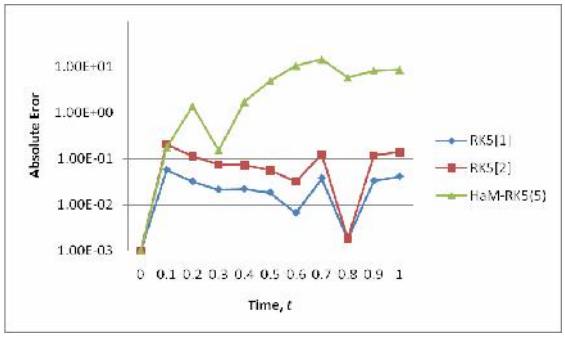

Fig. 3. Absolute error of all methods for z

From the graphs it can be seen that RK5[1] gives a better accuracy for x , y and z-directions where the absolute error from time steps Δt = 0.01 to Δt = 0.001 for each direction are less as compared to RK5[2] and HaM-RK5[5].

For a chaotic system r = 28, it can be seen that once again RK5[1] shows a better accuracy as compared to the other two methods for time steps Δt = 0.01 and Δt = 0.001. This can be observed from Tables 4-6 and Figs. 4-6 below:

Table. 4. x-direction differences among all methods for $r = 28$

t	x		
	$RK5[1]_{0.01}$-$RK5[1]_{0.001}$	$RK5[2]_{0.01}$-$RK5[2]_{0.001}$	HaM-$RK5[5]_{0.01}$- HaM-$RK5[5]_{0.001}$
0	0.00E+00	0.00E+00	0.00E+00
0.1	4.52E-02	1.53E-01	1.27E-01
0.2	2.78E-02	9.73E-02	1.42E+00
0.3	1.60E-03	8.93E-03	2.10E+00
0.4	2.99E-03	5.94E-03	3.19E+00
0.5	2.17E-03	3.37E-04	5.87E+00
0.6	4.72E-03	2.57E-02	1.20E+01
0.7	2.88E-02	9.64E-02	2.26E+01
0.8	4.48E-02	1.62E-01	2.79E+01
0.9	7.31E-02	2.50E-01	1.70E+01
1	3.87E-02	1.29E-01	5.39E+00

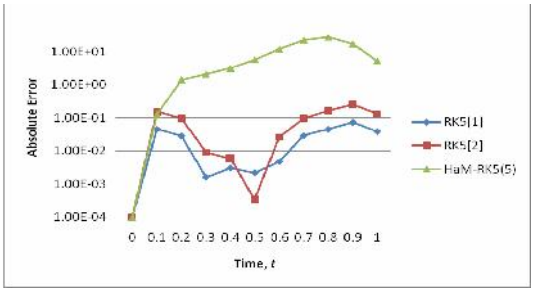

Fig. 4. Absolute error of all methods for x

Table. 5. y-direction differences among all methods for $r = 28$.

t	x		
	$RK5[1]_{0.01}$-$RK5[1]_{0.001}$	$RK5[2]_{0.01}$-$RK5[2]_{0.001}$	HaM-$RK5[5]_{0.01}$-HaM-$RK5[5]_{0.001}$
0	0.00E+00	0.00E+00	0.00E+00
0.1	5.49E-02	1.84E-01	1.77E-01
0.2	6.88E-02	2.33E-02	2.24E+00
0.3	4.82E-03	1.44E-03	2.76E+00
0.4	7.03E-03	2.69E-03	4.79E+00
0.5	2.28E-03	1.81E-04	9.76E+00
0.6	1.60E-03	6.72E-02	2.04E+01
0.7	9.16E-02	2.07E-02	3.31E+01
0.8	1.26E-02	4.33E-01	2.56E+01
0.9	3.88E-02	1.24E-01	3.04E+01
1	2.10E-02	6.60E-01	2.13E+00

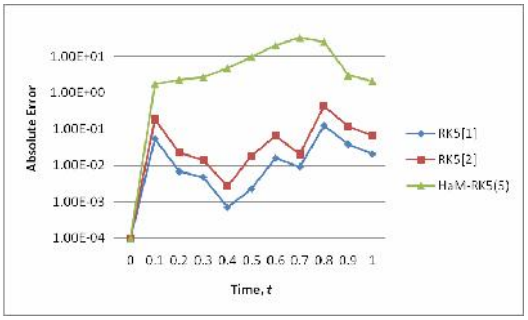

Fig. 5. Absolute error of all methods for y

Table. 6. z-direction differences among all methods for $r = 28$

t	x		
	$RK5[1]_{0.01}$-$RK5[1]_{0.001}$	$RK5[2]_{0.01}$-$RK5[2]_{0.001}$	HaM-$RK5[5]_{0.01}$-HaM-$RK5[5]_{0.001}$
0	0.00E+00	0.00E+00	0.00E+00
0.1	4.64E-02	1.64E-01	2.37E+00
0.2	4.73E-02	1.65E-01	7.94E+00
0.3	3.08E-03	1.08E-01	5.19E+00
0.4	2.40E-03	8.23E-02	7.00E+00
0.5	2.06E-02	6.58E-02	1.67E+00
0.6	1.31E-02	2.77E-02	5.58E+00
0.7	6.82E-02	2.48E-01	1.46E+00
0.8	2.22E-03	1.09E-02	5.57E+00
0.9	8.20E-02	2.87E-01	8.29E+00
1	6.60E-02	2.28E-01	6.48E+00

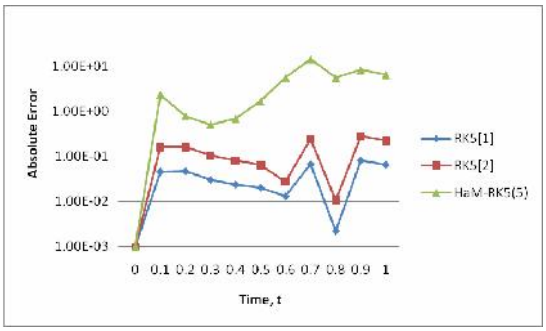

Fig. 6. Absolute error using RK5[1] on $\Delta t = 0.01$ for $r = 28$

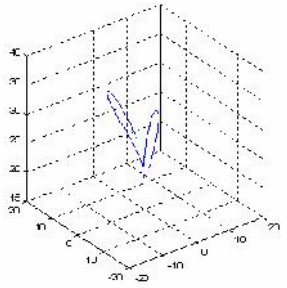

Fig. 7. Phase portrait using RK5[1] on $\Delta t = 0.01$ for $r = 23.5$

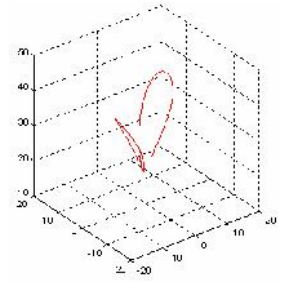

Fig. 8. Phase portrait using RK5[1] on $\Delta t = 0.01$ for $r = 28$

The xyz-phase portrait using RK5[1] on $\Delta t = 0.01$ for $r = 23.5$ is shown in Fig. 7. Figure 8 shows the xyz-phase portrait of the chaotic Lorenz system[5] using the RK5[1] on $\Delta t = 0.01$ for $r = 28$.

IV. Dynamical Behavior of Lorenz Model

The Jacobian matrix gives

$$\begin{bmatrix} \dot{X} \\ \dot{Y} \\ \dot{Z} \end{bmatrix} = \begin{bmatrix} -\sigma & \sigma & 0 \\ r - Z & -1 & -X \\ Y & X & -b \end{bmatrix} \begin{bmatrix} X \\ Y \\ Z \end{bmatrix}$$

and setting the determinant minus $\lambda \mathrm{I}$ equal to zero gives the eigenvalues as solutions of

$$\lambda^3 + (b + \sigma + 1)\lambda^2 + (b + b\sigma + \sigma - r\sigma + \sigma Z + X^2)\lambda + b\sigma(1 - r) + \sigma(XY + X^2 + bZ) = 0.$$

If the equilibrium point is taken to be the origin, this simplifies to

$$\lambda^3 + (b+\sigma+1)\lambda^2 + (b + b\sigma + \sigma - r\sigma + \sigma Z + X^2)\lambda + b\sigma(1-r) = 0.$$

Since b is clearly a solution, we get $(\lambda + b)\left(\lambda^2 + (\sigma+1)\lambda + \sigma(1-r)\right) = 0$,

and the three eigenvalues are:

$$\lambda_1, \lambda_2 = \frac{-\sigma - 1 \pm \sqrt{(\sigma+1)^2 + 4\sigma(r-1)}}{2},$$

$\lambda_3 = -b$, expressed in such a way to make it clear that $\lambda_1 > 0, \lambda_2, \lambda_3 < 0$ for $r > 1$. Thus the origin becomes unstable[6]. This is generally called a saddle, with a one-dimensional, unstable manifold. The eigenvalues of a linearization near the solutions of

$$\mu^3 + \mu^2(\sigma + b + 1) + \mu b(\sigma + r) + 2\sigma b(r-1) = 0.$$

Let b = 8/3 and σ = 10, then all three roots have negative real part if

$$r < \frac{\sigma(\sigma + b + 3)}{\sigma - b - 1} = \frac{470}{19} = r_H.$$

For $r < r_H$, the two complex eigenvalues have positive real part, and the equilibrium become unstable[6]. At $r = r_H$, there is a sub critical Hopf bifurcation.

For the values 99.524 < r < 100.795, there exists a period doubling window. The first period doubling, listed in increasing order of period, occurs at $r \approx 99.98$. Just above this bifurcation value, trajectories approach a stable periodic orbit that circles the first equilibrium once, then the second equilibrium twice, which we will denote [1-2-2], as in Fig. 9. As r decreases, the period doubles to [1-2-2-1-2-2] for 99.629 < r < 99.98 (Fig. 10). As r continues to approach the lower boundary of this window, 99.524, there is a cascade of period doubling similar to the behavior of chaotic one-dimensional maps. For 99.547 < r < 99.629 there is a period of [1-2-2], for 99.529 < r < 99.547 there is a period of [1-2-2], in Figs. 11 and 12 respectively.

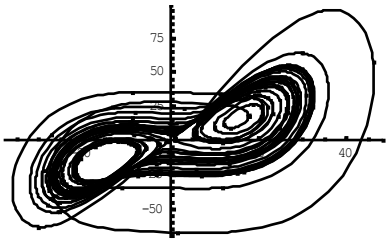

Fig. 9. Stable periodic orbit for r = 100.5

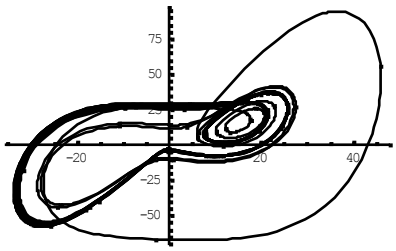

Fig. 10. Stable periodic orbits after the first period doubling, for r = 99.7

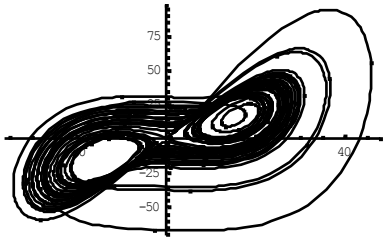

Fig. 11. Stable periodic orbit after the second period doubling, for r = 99.6

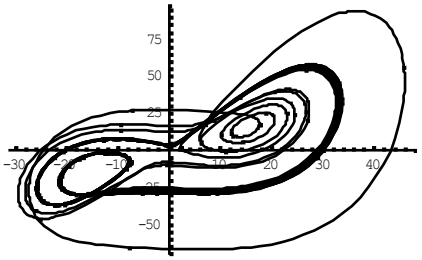

Fig. 12. Stable periodic orbit after the third period doubling, for r = 99.537

In general, the period doubling cascades have the same properties as in scalar maps, such as the Feigenbaum number, $\delta = \lim_{n\to\infty} \frac{r_{n+1} - r_n}{r_{n+2} - r_{n+1}} = 4.669....$ which can be

used to find the accumulation value r_∞. The behavior in the upper half of the period doubling window is interesting as well. The fact that the window has an upper bound suggests that the system demonstrates non-periodic behavior once again as *r* exceeds it. This is true, and the transition can be seen through what is called intermittent chaos. This phenomenon is shown in Fig. 13 for *r* = 100.93. As time progresses, the trajectory tends toward the periodic orbit, but so often it lapses into non-periodic, chaotic behavior for an interval of time. If *r* is within the period doubling window, the intermittent chaos will eventually cease, leaving a periodic orbit, but once *r* is beyond the upper bound r_c, intermittent chaos will occur after any given time. As *r* moves further from the window, the periods of intermittent chaos will increase in length until they dominate the trajectory.

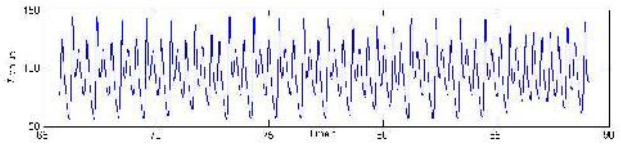

Fig. 13. Intermittent chaos just above the period doubling window for *r* = 100.93

There exist two other period doubling windows as *r* increases. The first is 145 < *r* < 166. For 154.4 < *r* < 166.07 there is a stable symmetric periodic orbit with a period described by [1-1-2-2]. At *r* ≈ 154.4 the stable symmetric orbit splits into two stable asymmetric periodic orbits with periods described by [1-1-2-2], producing between them an unstable periodic orbit. These orbits undergo simultaneous period doubling bifurcations as *r* decreases in a manner similar to that of the first window[7]. The final period doubling window is for 214.364 < *r*, with period described by a symmetric stable [1-2] orbit. This window is similar to the previous, except that for *r* > 313, the lowest period orbit continues to exist.

Conclusion

The Lorenz model is highly sensitive to the initial conditions of the system, but nevertheless falls into an overall pattern as time increases regardless of initial condition. In this paper, all three methods applied to the Lorenz system when the system is chaotic and non-chaotic. For both cases, it is proved that the modified fifth-order Runge-Kutta method appears to be the best method to approximate this solution based on its accuracy.

---

1. Lorenz E., 1963, Deterministic nonperiodic flow, *J. Atmos. Sci.* 20:130-141.
2. Randall, D.A., 1994, The Navier-Stokes Equation, Department of Atmospheric Science, Colorado State University, Fort Collins, Colorado.
3. Cartwright, J.H.E. & O. Piro, 1992, The Dynamics of Runge-Kutta methods, *Int. Bif. & Chaos,* 2: 427- 449.
4. Yaacob, N. & B. Sanugi, 1995, A New Fifth-Order Five-Stage Explicit HaM-RK5(5) Method for Solving Initial Value Problems in ODE's, Laporan Teknik. Jab. Mat., UTM.
5. Razali, N. & R. Ahmed, 2008, New Fifth-order Rung-Kutta Methods for solving Ordinary Differential Equations, *Proc. Seminar of Engineering Math*., 2, 155-162.
6. Hale, J. and H. Kocak, 1991, Dynamics and Bifurcations, Springer-Verlag, New York.
7. Sparrow, C., 1982, The Lorenz Equations: Bifurcations, Chaos, and Strange Attractors, Springer-Verlag, New York.